Korean J. Chem. Eng., 32(1), 43-50 (2015)
DOI: 10.1007/s11814-014-0181-5

pISSN: 0256-1115
eISSN: 1975-7220

Application of Hilbert-Huang transformation in fluidized bed with two-component (biomass particles and quartz sands) mixing flow

Xiaoyi Wang, Zhaoping Zhong†, Heng Wang, and Zeyu Wang

Key Laboratory of Energy Thermal Conversion and Control of Ministry of Education,
School of Energy and Environment, Southeast University, Nanjing 210096, China
(*Received 29 May 2014 • accepted 27 June 2014*)

Abstract−Hilbert-Huang transformation was used to investigate the nonlinear characteristics of two-component (biomass particles and quartz sand) mixing flow by analyzing the pressure fluctuation signals in fluidized bed. Based on empirical mode decomposition (EMD), the Hilbert-Huang spectra in bubbling and slugging flow patterns were obtained and analyzed. In bubbling flow pattern, compared with one-component (quartz sand) flow, the energy of two-component mixing flow is lower in 0-5 Hz and higher in 40-50 Hz. In slugging flow pattern, the energy in pressure fluctuation mainly lies in 0-5 Hz. and the effect of biomass particles on the Hilbert-Huang spectrum is not very obvious. Compared with traditional power spectral density (PSD), HHT is much more suitable for investigating pressure fluctuation signals in fluidized beds.

Keywords: Fluidized Bed, Biomass Particle, Empirical Mode Decomposition, Hilbert-Huang Transformation, Pressure Fluctuations

INTRODUCTION

Biomass is widely considered as clean energy by researchers. Biomass gasification is an effective method to utilize the biomass energy, which can reduce not only the use of fossil fuel but also the emissions of pollutant. Fluidized biomass gasification with the high mixing efficiency between particles and gas is an essential process for the conversion of biomass energy [1,2]. However, biomass particles have some properties (e.g., low density, soft texture and extreme shapes), which makes them difficult to be fluidized. Inert particles, such as quartz sand, are used as fluidization medium to improve fluidization efficiency. The mixing flow of biomass and fluidization medium in fluidized bed has been studied by researchers. Clarke et al. [3] investigated the mixing flow of glass balls and wood with different moisture content in fluidized beds. Shao et al. [4] researched the minimum fluidization velocity of particles with different shapes and densities when mixing with quartz sand in fluidized bed. And some other researchers focused on the effects of catalyst [5,6].

However, traditional biomass particles have the properties which can make them be easily separated from fluidizing medium. So the compression molding process is used to shape the biomass. Compressed biomass particles widely used in industry have properties like high density, regular shape and easy storage. But the size of particles is larger than fluidizing medium, which would have a great influence on the flow. It is necessary to study the hydrodynamic characteristics of mixed flow with compressed biomass particles and fluidizing medium in fluidized bed, and now this regard has rarely been reported.

†To whom correspondence should be addressed.
E-mail: zzhong@seu.edu.cn

The pressure fluctuation signals are easy to measure with low price, which is practicable in industrial application [7]. So many researchers have used pressure fluctuation signals to analyze the flow hydrodynamic characteristics about bubble behaviors and particle flow in a fluidized bed [8-10]. In recent years, the Hilbert-Huang transformation (HHT) has been considered to be a major breakthrough to deal with nonlinear and non-stationary signals as the results are derived from the signal itself, which could be adaptive. This method has been applied to deal with the pressure fluctuation signals of gas-liquid and gas-solid flow. HHT is an effective method to analyze the pressure fluctuation signals, which has been proposed by Ding et al. [8] and Luo et al. [11], and it also can be used to analyze the distribution of energy-frequency-time quantitatively. Briongos et al. [12] applied HHT to characterize hydrodynamic behavior in a fluidized bed, and the chaotic characteristics of the system.

In this paper, the mixed flow of compressed biomass particles and quartz sand was researched and compared with mono-flow of quartz sand, which is the traditional hard particles flow of one-component. HHT analysis was used to research the distribution of energy-frequency-time of the system, the hydrodynamic behavior of two-component flow and the influence of biomass particles on the flow characteristics, e.g., bubble and particle flow, which has practical significance in enhancing heat transfer and improving the efficiency of biomass pyrolysis and gasification.

EXPERIMENT

The experimental system, shown in Fig. 1, consists of a fluidized bed in a laboratory scale, gas supply system, data acquisition system and image collection system. The fluidized bed is made of 6 mm thick Plexiglas, with a height of 1,000 mm. A larger aspect ratio was used to observe the characteristics of bubble and particle flow in

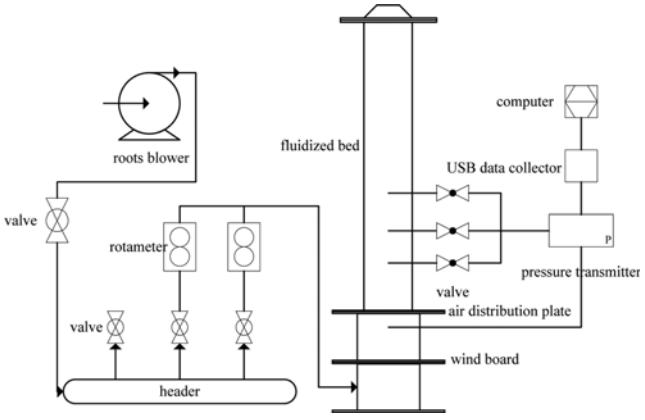

Fig. 1. Experimental system of the fluidized bed.

this research, and the section size was 120×32 mm. The air distribution plate, which is arranged with 126 circular holes in equilateral triangles, is 6 mm in thickness. The diameter of circular holes is 1 mm and the opening ratio is 2.6%. There is a 60 mesh screen on the air distribution plate to prevent the holes blocking. The fluidizing air is provided by a roots blower, and the air volume is controlled by a rotameter. A wind board is used to make the measured pressure fluctuation more accurate.

Considering that the pressure detecting points should be arranged at the place where fluidization fully developed [13], there are three pressure detecting points in different heights, located on the center of the wall at the height of 200 mm, 300 mm, 400 mm over the air distribution plate, respectively. The pressure fluctuation signals are measured by differential pressure transmitter (the type is KMSSTO, and the measuring range of the sensor is 0-35 kPa) and USB data collector (RBH8251-13). A sensor is installed on the test bench, and the rubber tube is used to connect sensor to the fluidized bed. The sampling frequency is f=100 Hz, and the sampling time is t≈ 10 s (the number of sampling points n=1024).

In the experiments, quartz sand and compressed cylindrical biomass particles are used as the bed materials, shown in Fig. 2, respectively. The average particle size of quartz sand is 0.8 mm, and the density is 2,650 kg/m^3. Both the length and diameter of the cylinder-shaped biomass particles are 10 mm, and the density is about 1,300 kg/m^3. The mass proportion of biomass is w, and the initial height of fluidized bed is H. The flow will layer easily if the proportion of biomass particles is too large, but it will reduce the utilization efficiency of biomass when the proportion becomes small. Considering that the volume ratio of biomass particles and quartz sand is 1 : 4 in our research. The minimum fluidization velocities of one-component and two-component flow were 0.87 m/s and 0.92 m/s, as measured by velocity reducing method.

ANALYSIS METHODS

Hilbert-Huang transformation is a method for analyzing nonlinear and non-stationary processes developed by Huang et al. in 1998 [14], and then the solution and distribution of Hilbert-Huang spectrum were further described [15,16]. HHT includes two main steps: empirical mode decomposition (EMD) and Hilbert transformation (HT). The core part of HHT is EMD. First, EMD is used to extract intrinsic mode functions (IMFs) from the signals. Second, Hilbert transform is applied to each of the IMF components. Finally, the instantaneous frequency and amplitude can be calculated.

IMFs are extracted from the signals based on EMD [14,15], which reflect the characteristic information of the original signal.

The original time series x(t) can be exactly reconstructed by IMFs and a residue $r_k(t)$ which could be calculated by the following linear combination:

$$x(t)=\sum_{i=1}^{k} I_i(t)+r_k(t) \tag{1}$$

where $I_i(t)$ is IMF component, and k is the total number of IMFs, and $r_k(t)$ is the residue of signal x(t) after the sifting process, which represents the trend of x(t).

To calculate the instantaneous frequency, Hilbert transform [17] is applied for each IMF, and $H_i(t)$ is obtained:

$$H_i(t)=\frac{1}{\pi}C\int_{-\infty}^{+\infty}\frac{I_i(\tau)}{t-\tau}d\tau \tag{2}$$

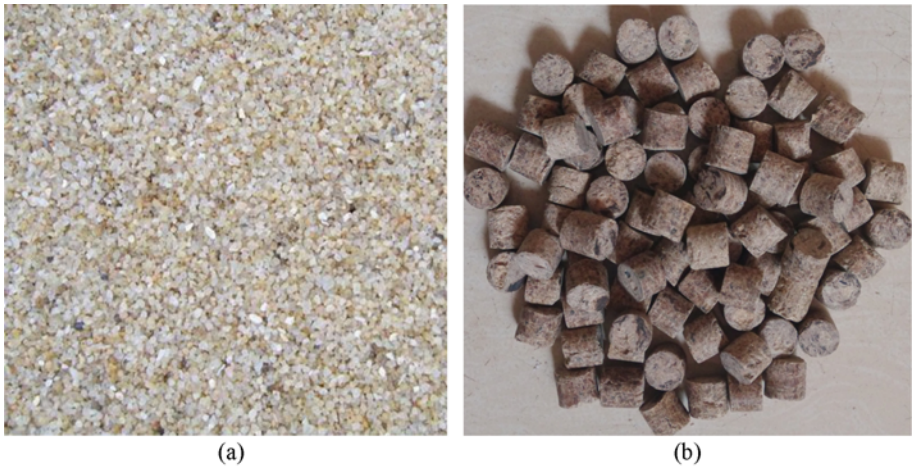

(a) (b)

Fig. 2. Bed materials (a) quartz sand; (b) biomass particles.

where, C is Cauchy principal value, and C is chosen as 1 in this manuscript. Then, an analytical signal $Z_i(t)$ can be constructed by $I_i(t)$ and $H_i(t)$:

$$Z_i(t) = I_i(t) + jH_i(t) = a_i(t)e^{j\theta_i(t)} \quad (3)$$

where, the amplitude (t) and the phase $\theta_i(t)$ can be calculated by the following:

$$a_i(t) = \sqrt{I_i^2(t) + jH_i^2(t)} \quad (4)$$

$$\theta_i(t) = \arctan\left(\frac{H_i(t)}{I_i(t)}\right) \quad (5)$$

The instantaneous frequency $w_i(t)$ of the analytic signal $Z_i(t)$ is determined by the phase:

$$w_i(t) = \frac{d\theta_i(t)}{dt} \quad (6)$$

Thus, the original time series x(t) can be expressed by the instantaneous frequency and the amplitude of all analytical signals:

$$x(t) = \mathrm{Re}\sum_{i=1}^{k} a_i(t)e^{j\int w_i(t)dt} \quad (7)$$

The weighted amplitude of instantaneous frequency can be shown in time-frequency plane, and that is a three-dimensional plot of time-frequency-energy called Hilbert-Huang spectrum H(w, t).

Then the marginal spectrum, which integrates the Hilbert-Huang spectrum along the time axis, can be defined as:

$$h(w) = \int_0^T H(w,t)dt \quad (8)$$

where, T is the total data length. The marginal spectrum offers the contribution of the total amplitude at each frequency.

Hence, to analyze the change among each IMF component and the proportion of IMF in original signals, we define the energy of IMF as follows:

$$E_k = \sum_{i=1}^{n} \left| a_i^2(t) \right| \quad (9)$$

RESULTS AND DISCUSSION

1. Time Domain Analysis of Intrinsic Mode Functions

In this paper, bubbling pattern and slugging pattern are analyzed, and the snapshots of these tow patterns are shown in Fig. 3. The EMD method was used to extract IMF1-IMF7 from the original pressure fluctuation signals. Fig. 4 shows the IMF components for the pressure fluctuation signals in the fluidized bed when the superficial gas velocity is 1.3 m/s. The original time series, I_0, is plotted on the top row of the figure, and I_1-I_7 show the IMFs from high-frequency to low-frequency. The frequency of each IMF is lower than the preceding one, because each step of the EMD method extracts the highest frequency component from the signals. The EMD is adaptive, and the IMF components reflect the authenticity of signals, which is very distinct from other methods. From Fig. 4, the IMFs with irregular wave shape all exhibit frequency modulation and amplitude modulation properties; this is the expression of non-linear characteristic in fluidized bed, which results from interaction between gas and particle phases.

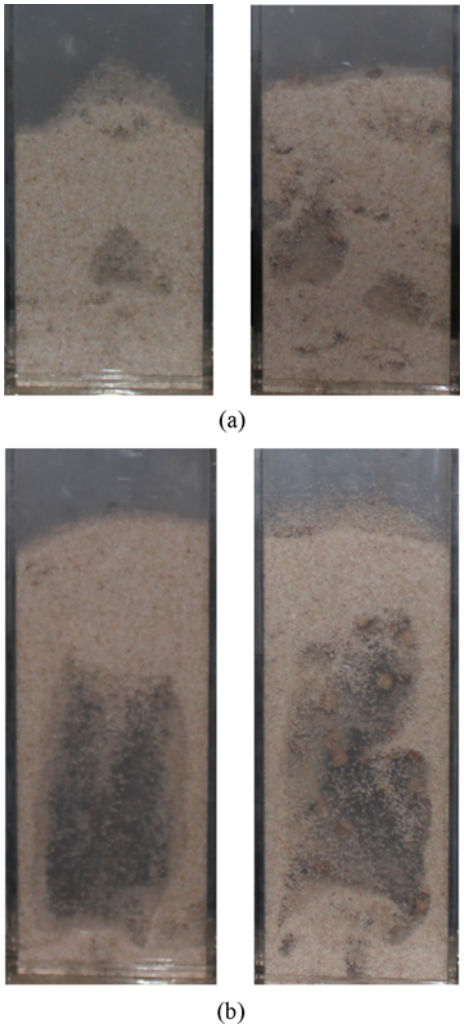

Fig. 3. Photos of different pattern with quartz sand alone and biomass particles and quartz sand mixed flow: (a) bubbling pattern (H=150 mm, w=6.4%, u=1.30 m/s) (b) slugging pattern (H=150 mm, w=6.4%, u=2.31 m/s).

2. Hilbert-Huang Spectrum Analysis

Several typical Hilbert-Huang spectra of pressure fluctuation signals are shown in Fig. 5 and Fig. 6, where the abscissa and ordinate indicate the sampling time and instantaneous frequency, respectively. The Hilbert-Huang spectrum is encoded as a color scale map, and the color bar denotes that the time and frequency depend on normalized energy; meanwhile, the color ranging from black to white indicates the energy changing from the minimum to the maximum value [14,15]. In the Hilbert-Huang spectrum for pressure fluctuation signals, the color is not continuous and not stationary, which illustrates the amplitude of the pressure fluctuation is non-stationary. The non-stationary characteristic results from particle distribution and the change of particles with different velocities in vertical and axial [18].

Fig. 5(a) shows the Hilbert-Huang spectrum for one-component flow in bubbling pattern, and the energy-frequency-time dis-

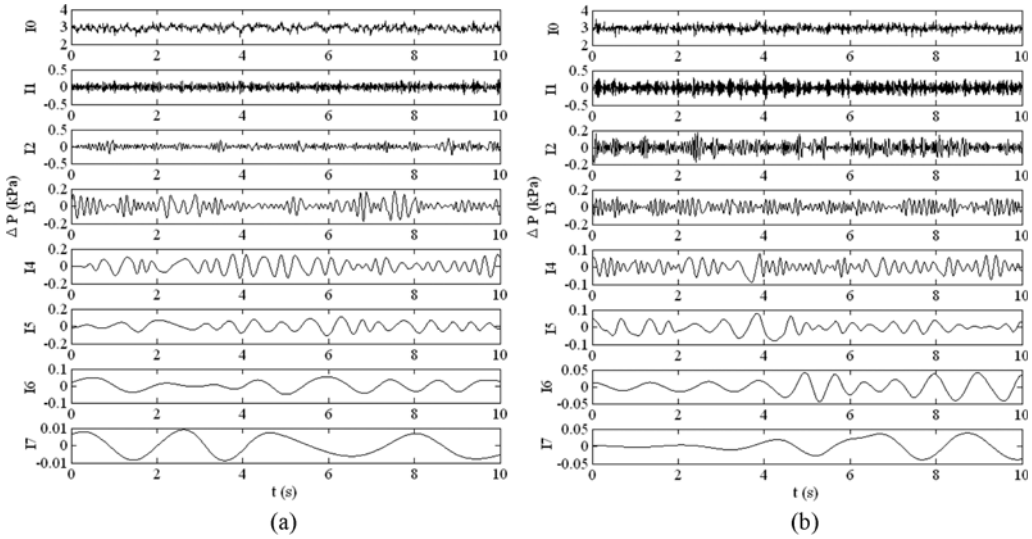

Fig. 4. IMF components of the pressure fluctuation signal at 1.3 m/s (H=150 mm, w=6.4%).
(a) Two-components mixed flow (b) One-component flow

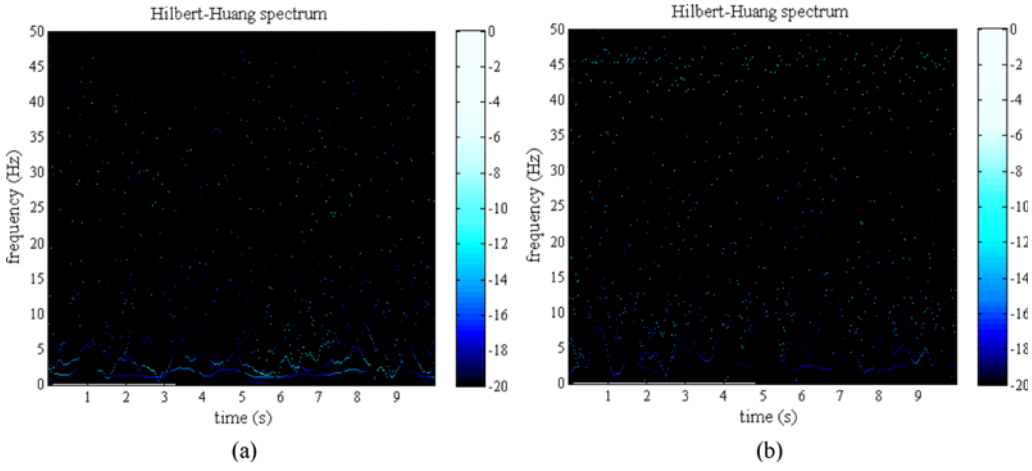

Fig. 5. Hilbert-Huang spectrums of two kinds of compositions under bubbling pattern (H=150 mm, w=6.4%, u=1.30 m/s).
(a) One-component (b) Two-components

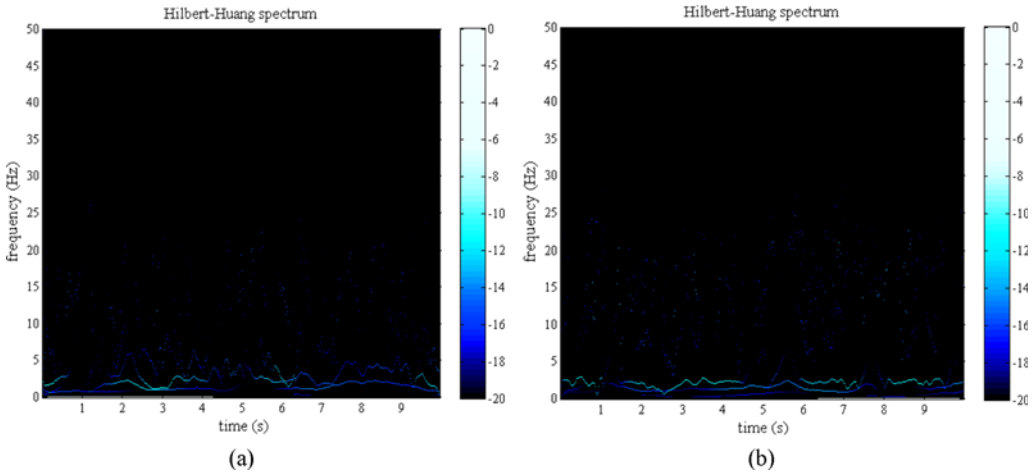

Fig. 6. Hilbert-Huang spectrum of two kinds of compositions under slugging pattern (H=150 mm, w=6.4%, u=2.31 m/s).
(a) One-component (b) Two-components

tributions of pressure fluctuation signals. In low frequency region (<5 Hz), the instantaneous frequency is continuous, and the energy is high. That is because the bubbles are relatively stable and show a periodic characteristic in this condition [8]. There is a part of energy distribution still lying in middle and high frequency regions (>5 Hz), which is caused by the movement of bubbles with different sizes and velocities. The Hilbert-Huang spectrum of two-component mixing flow in bubbling pattern is plotted in Fig. 5(b). In this condition, the energy distribution is rare in 0-5 Hz, and the distribution of frequency is consistent with that of energy. Compared with the one-component flow, the instantaneous frequency for two-component flow is discontinuous, and the energy is located in the region where frequency is larger than 20 Hz.

The bubble size increases with the increase of the gas velocity. Because the cross section of the fluidized bed is small in this research, a slugging pattern can be observed when the gas velocity is large enough. Fig. 6 shows the Hilbert-Huang spectrum of pressure fluctuation signals in the slugging pattern. Compared with the bubbling pattern, the bubble size in the slugging pattern is much larger, which makes the Hilbert-Huang spectrum very distinct from that in bubbling pattern. In the slugging pattern, the frequency of signals lies between 0 Hz to 5 Hz, and the energy is also concentrated in this range. Only a little of the energy and frequency lies between 5 Hz to 25 Hz, and there is almost no energy and frequency above 25 Hz. The Hilbert-Huang spectra for one-component flow and two-component mixing flow have similar characteristic. It illustrates that the pressure fluctuation is mainly influenced by the bubble formation and break, while the influence of biomass particles is very small.

3. Discussion of Marginal Spectrum and Power Spectral Density (PSD) for Pressure Signal Analysis

The frequency characteristic of pressure fluctuation in a fluidized bed was also analyzed by fast Fourier transform (FFT), and the power spectral densities (PSD) can be obtained [19-21]. In the FFT, the energy of the frequency means a component of a sine or a cosine wave persisted through the time span of the data [22], which is a stationary and linear analysis. So, the traditional FFT technique is not very suitable for analyzing the pressure fluctuation signals [23]. Compared with PSD, the marginal spectrum is non-stationary and nonlinear. Additionally, the marginal spectrum is local and certainty, which is very different from the frequency of PSD [24].

To compare the differences between marginal spectrum and PSD

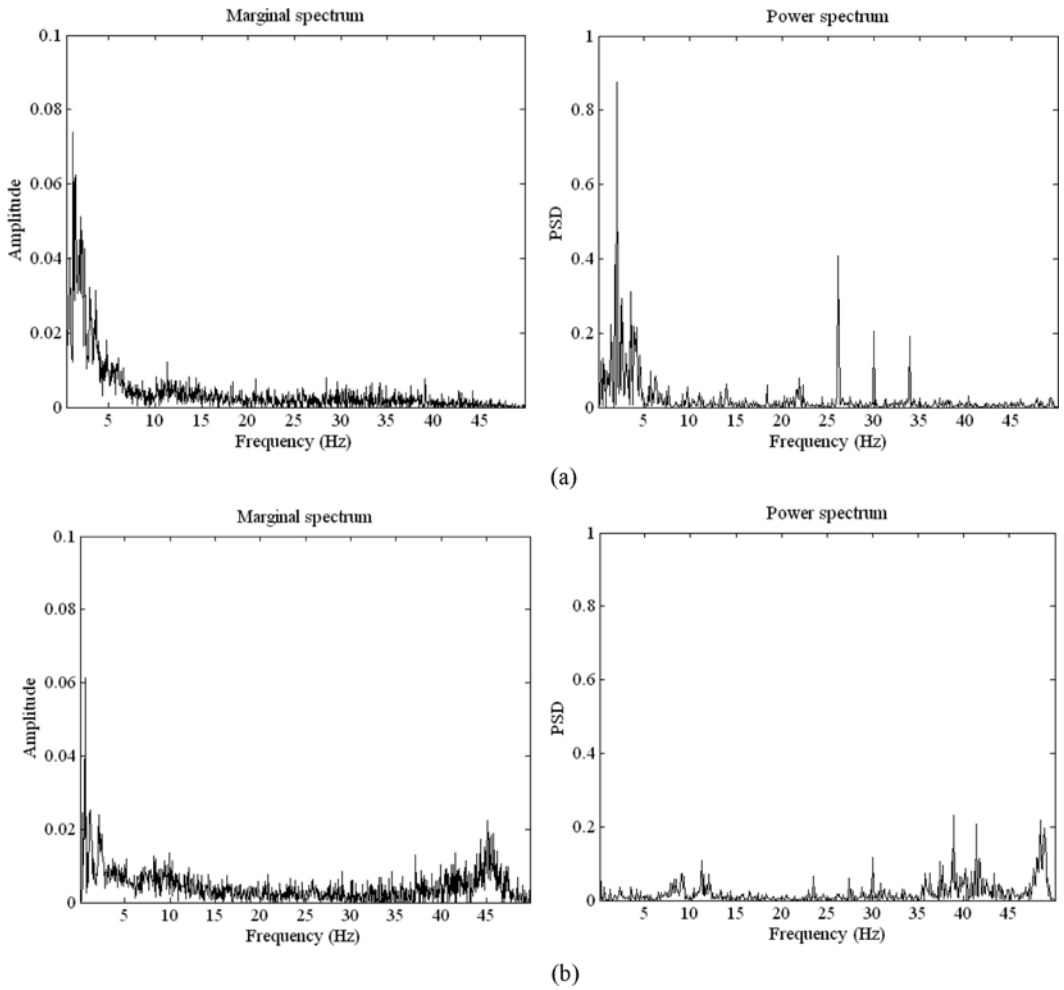

Fig. 7. Marginal spectra and PSD of two kinds of compositions under bubbling pattern (H=150 mm, w=6.4%, u=1.30 m/s).
(a) One-component flow (quartz sand); (b)Two-component mixing flow (biomass particles and quartz sand)

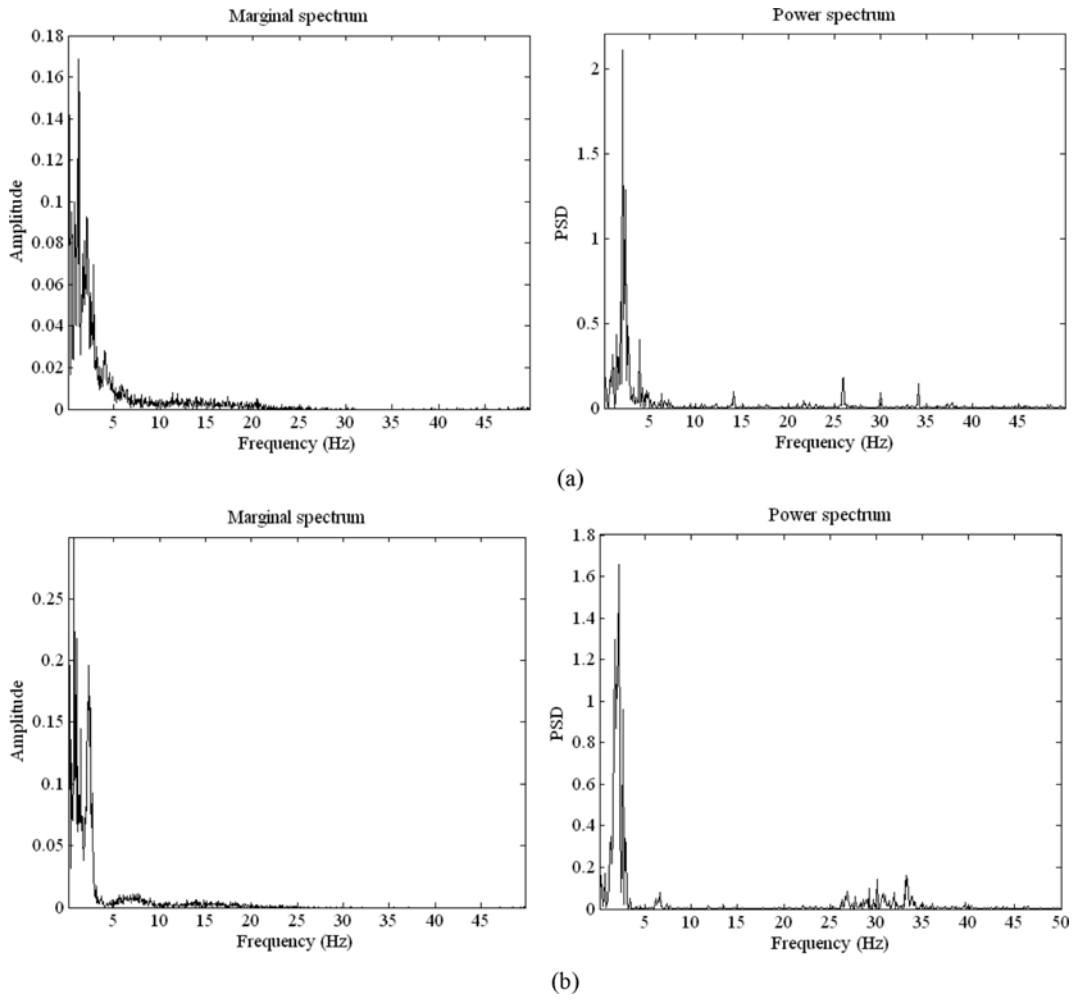

Fig. 8. Marginal spectra and PSD of two kinds of compositions under slugging pattern (H=150 mm, w=6.4%, u=2.31 m/s).
(a) One-component flow (quartz sand); (b)Two-component mixing flow (biomass particles and quartz sand)

for pressure signal analysis, the marginal spectrum and PSD in bubbling pattern and slugging pattern are shown in Fig. 7 and Fig. 8, respectively. Both the marginal spectrum and PSD can reflect the change of the flow pattern, and the energy distributions in the marginal spectrum and PSD are similar. However, the frequency distributions in the marginal spectrum and PSD are very different, which is due to the restrictions of linearity and stationary assumptions by FFT. When analyzing the pressure fluctuation signals with FFT method, the linear superposition of trigonometric function is used and many additional harmonic components are added to simulate the inherent features of the signals [24]. The additional harmonic may have misleading results, which cannot accurately reflect the true frequency-energy distribution for pressure fluctuation signals in a fluidized bed. The marginal spectrum of the signals indicates the accurate frequency-energy distribution, and there are no additional harmonics in the marginal spectrum.

From Fig. 7, compared with one-component flow, the energy amplitude between 0 Hz and 5 Hz is low, but it is high from 40 Hz to 50 Hz in two-component mixing flow. In summary, the frequency distribution is relatively homogeneous in two-component mixing flow. The spectra of slugging pattern are shown in Fig. 8, the marginal spectra are shown in the left, and they present similar characteristics that the high energy amplitude lies in 0-5 Hz and almost no amplitude lies above 25 Hz. The energy amplitude decreases with the frequency scales from 5 Hz to 25 Hz, which could be found in PSD. The marginal spectrum provides better results than the power spectrum.

4. Energy Characteristics Extracted

The energy of each IMF at different gas velocities was calculated to analyze the relationship between energy distribution and the gas velocity [9]. The energy of IMFs for one-component and two-components mixing flow is shown in Table 1 and Table 2, respectively. E1, the energy of highest frequency, is higher in two-component mixing flow than that in one-component flow.

Based on the previous research data and literatures published [8, 18,25], the frequency of big bubble is mainly in 1-5 Hz, so the IMFs are divided into three frequency bands, and the percentage of the energy for each band is expressed by P. $P_{1\sim2}$ is the percentage of E1 and E2 in high-frequency band (>25 Hz), $P_{3\sim5}$ is the percentage of E3, E4 and E5 in middle-frequency band (5-25 Hz), and $P_{6\sim7}$ is the percentage of E6 and E7 in low-frequency band (<5 Hz). Fig. 9 shows the energy ratio distribution in different frequency

Table 1. The energy of IMFs for one-component flow in fluidized bed at different superficial gas velocities (H=150 mm, w=6.4%)

Gas velocity (m/s)	Flow pattern	E1	E2	E3	E4	E5	E6	E7
0.87	Bubble	7.1236	8.0801	2.5021	0.9352	0.1669	0.2127	0.0381
1.01	Bubble	6.2017	5.8631	3.4270	0.9738	0.449	0.6553	0.0999
1.15	Bubble	6.1328	3.9199	3.3066	3.9835	2.0604	0.7664	0.0317
1.3	Bubble	6.7234	2.5501	3.3423	5.6982	2.5917	0.2961	0.0279
1.45	Bubble	6.2215	1.9618	2.8629	6.4522	4.5918	0.5802	0.01121
1.74	Slug	2.788	2.3881	3.4865	8.6929	5.0617	0.9999	0.03269
2.02	Slug	1.7504	2.6046	5.0773	15.8769	9.4857	1.6437	0.4129
2.31	Slug	1.365	2.5475	4.8651	21.0683	9.7354	1.7456	2.1376

Table 2. The energy of IMFs for two-components flow in fluidized bed at different superficial gas velocities (H=150 mm, w=6.4%)

Gas velocity (m/s)	Flow pattern	E1	E2	E3	E4	E5	E6	E7
0.87	Bubble	15.3127	3.2588	1.2520	1.4831	0.3538	0.1559	0.0539
1.01	Bubble	18.4488	4.3607	3.0125	1.2129	0.4185	0.1581	0.1006
1.15	Bubble	17.123	3.0043	2.3499	0.9283	0.8657	0.3912	0.3716
1.3	Bubble	18.1746	3.8512	1.9510	1.1013	1.3363	1.7964	0.3781
1.45	Bubble	19.6964	3.8939	1.1630	2.3936	2.1971	0.9108	0.7271
1.74	Slug	8.5803	2.8587	1.2035	18.9766	4.7800	1.1363	0.2657
2.02	Slug	5.4578	2.4896	7.4221	22.1197	13.4451	0.8902	2.6272
2.31	Slug	4.6342	3.1327	4.4397	36.6837	10.0436	4.5199	0.9775

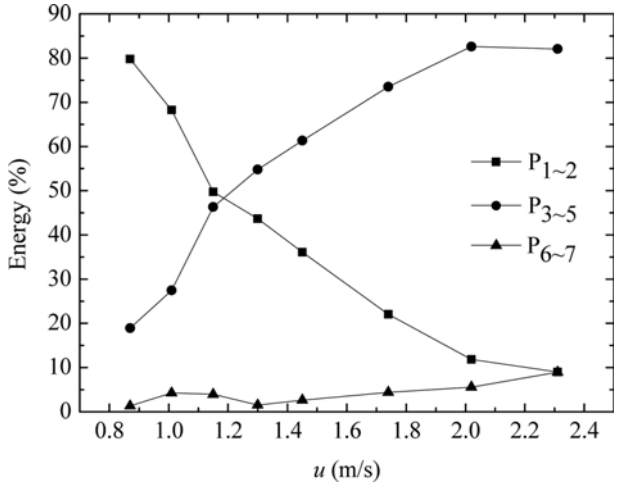

Fig. 9. Energy ratio distribution in different frequency bands of one-component flow (H=150 mm, w=6.4%).

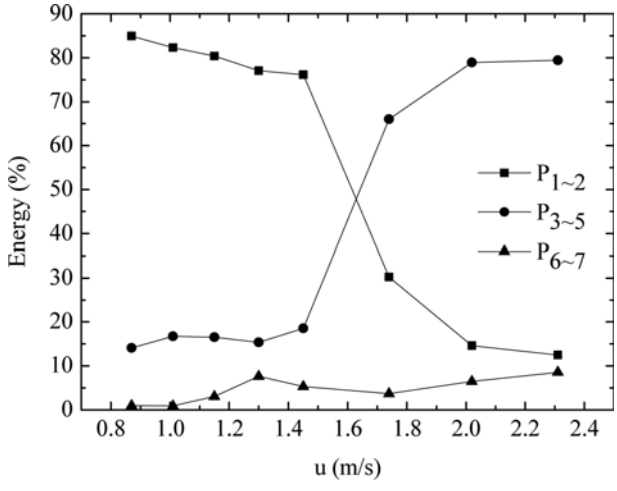

Fig. 10. Energy ratio distribution in different frequency bands of two-components flow (H=150 mm, w=6.4%).

bands of one-component flow. As the superficial gas velocity increases, the energy ratio of high-frequency band decreases gradually, but the energy ratio of middle-frequency band increases gradually. In gas-liquid two-phase flow, Ding et al. also reached a similar conclusion that the energy transfer from high-frequency band to middle-frequency band as the pattern is changing from bubble flow to slug flow [7]. The bubble size increases with the raise of gas velocity, and the effect of bubbles on the pressure fluctuation enhances with the growth of the bubble size [26]. So with the rising of the gas velocity, the energy decreases in the high-frequency band, but increases in the middle-frequency band.

The energy ratio distribution of two-component mixing flow is shown in Fig. 10. What is different from one-component flow is that, in bubbling pattern, the flow of quartz sand is disturbed by biomass particles, the number of random bubbles increases and the size of bubbles decreases. Consequently, the percentage of energy is mainly located in the high-frequency band, and the variation of energy ratio is not obvious in the condition as shown in Fig. 10. The energy ratio of the high-frequency band decreases, and the energy ratio of middle-frequency band increases rapidly when the slugging pattern appears. However, only a little proportion of energy is located in the low-frequency band, the energy ratio in slugging pattern is slightly higher than that in bubbling pattern, and the variation of energy ratio is slight, which is determined by the nonlinear

and non-stationary characteristics of pressure fluctuation in fluidized bed.

In summary, by the HHT analysis, in the bubbling pattern, the energies of two-component mixing flow mainly lie at high frequency, and the periodicity of the system is low. That is because the bubbles and quartz sand flow are affected by the disturbance of biomass particles. The bubbles, affected by biomass particles, disperse into different sizes in two-component mixing flow.

CONCLUSIONS

Two-component (quartz sand and biomass) mixing flow in a fluidized bed was investigated. To understand the nonlinear characteristics in fluidized bed deeply, the HHT method was used to analyze the pressure fluctuation signals. Different from the traditional spectrum analysis, the Hilbert-Huang spectrum can present instantaneous information of the energy and frequency.

To demonstrate the adaptive characteristic of HHT, the marginal spectrum was compared with the PSD. It was found that PSD could not reflect the energy distribution between 5 Hz and 25 Hz. Hence, the marginal spectrum provides better results than PSD, and PSD was not very suitable for the pressure signal analysis in fluidized bed.

The energy-frequency-time distributions of pressure fluctuation signals were analyzed. In the bubbling pattern, the frequency of two-component mixing flow is high and relatively homogeneous, and the energy in the high frequency band does not decrease as the gas velocity increases. In addition, the energy in the high frequency band is distributed uniformly. In the slugging pattern, the energy lies mainly between 0 Hz to 5 Hz, and the Hilbert-Huang spectra of one-component flow and two-component mixing flow are very similar. That illustrates that the effect of the biomass particles on the flow is not obvious. In conclusion, this study will lead to a better understanding of the flow characteristics of biomass particles and inert particle mixing flow.

ACKNOWLEDGEMENTS

This research is supported by the National Natural Science Fund Program of China (51276040), National Natural Science Fund Program of China (U1361115).

REFERENCES

1. P. M. Lv, Z. H. Xiong, C. Z. Chang, Y. Chen and J. X. Zhu, *Bioresour. Technol.*, **95**, 95 (2004).
2. B. Leckner and M. Karlsson, *Emission from circulating fluidized bed combustion of mixtures of wood and coal*, in: L. Rubow, G. Commonwealth (Eds.), *Proceedings of 1993 International Conference on Fluidized Bed Combustion*, American Society of Mechanical Engineers, New York, 109 (1993).
3. K. L. Clarke, T. Pugsley and G. Hill, *Chem. Eng. Sci.*, **60**, 6909 (2005).
4. Y. J. Shao, B. Ren and B. S. Jin, *Powder Technol.*, **234**, 67 (2013).
5. H. Y. Zhang, R. Xiao, B. S. Jin, D. K. Shen, R. Chen and G. M. Xiao, *Bioresour. Technol.*, **137**, 82 (2013).
6. Ofei D. Mante, F. A. Agblevor and R. McClung, *Fuel*, **108**, 451 (2013).
7. W. H. Zhang and X. G. Li, *Chem. Eng. Sci.*, **64**, 1009 (2009).
8. H. Ding, Z. Y. Huang, Z. H. Song and Y. Yan, *Flow Measurement and Instrumentation*, **18**, 37 (2007).
9. C. H. Wang, Z. P. Zhong and J. Q. E., *Powder Technol.*, **219**, 20 (2012).
10. C. D. Si, J. Zhou and Q. J. Guo, *Journal of the Taiwan Institute of Chemical Engineers*, **42**, 929 (2011).
11. L. J. Luo, Y. Yan, P. Xie, J. W. Sun, Y. Y. Xu and J. Q. Yuan, *Chem. Eng. J.*, **181-182**, 570 (2012).
12. J. V. Briongos, J. M. Aragón and M. C. Palancar, *Chem. Eng. Sci.*, **61**, 6963 (2006).
13. C. Alberto, S. Felipe and C. S. Rocha, *Chem. Eng. Res. Design*, **03**, 497 (2004).
14. N. E. Huang and Z. Shen, *Proceedings of the Royal Society of London, Series A*, **454**, 903 (1998).
15. N. E. Huang, *Stochastic Structural Dynamics*, 559 (1999).
16. N. E. Huang, M. C. Wu and S. R. Long, *Proceedings of the Royal Society of London*, **459**, 2317 (2003).
17. S. L. Hahn, *Hilbert Transforms in Signal Processing*, Artech House, Boston (1996).
18. P. Lu, D. Han, R. X. Jiang, X. P. Chen, C. S. Zhao and G. C. Zhang, *Exp. Therm. Fluid Sci.*, **51**, 174 (2013).
19. O. Jaiboon, B. Chalermsinsuwan, L. Mekasut and P. Piumsomboon, *Powder Technol.*, **233**, 215 (2013).
20. M. X. Liu, Y. M. Zhang, H. Bi, J. R. Grace and Y. D. Zhu, *Chem. Eng. Sci.*, **65**, 3485 (2010).
21. M. C. Shou and L. P. Leu, *Chem. Eng. Res. Design*, **83**, 478 (2005).
22. V. K. Rai and A. R. Mohanty, *Mechanical Systems and Signal Processing*, **21**, 2607 (2007).
23. N. E. Huang, Z. Shen, S. R. Long, M. C. Wu, H. H. Shih, Q. Zheng, N. C. Yen, C. C. Tung and H. H. Liu, *Proceedings of the Royal Society of London, Series A:Mathematical, Physical and Engineering Sciences*, **454**, 903 (1998).
24. Z. S. Yang, Z. H. Yu, C. Xie and Y. F. Huang, *Measurement*, **47**, 14 (2014).
25. X. P. Wang, *Journal of Chemical Engineering of Chinese Universities*, **19**, 474 (2005).
26. M. X. Liu, Y. M. Zhang, H. Bi, J. R. Grace and Y. D. Zhu, *Chem. Eng. Sci.*, **65**, 3485 (2010).